Scientific African 21 (2023) e01792

Contents lists available at ScienceDirect

Scientific African

journal homepage: www.elsevier.com/locate/sciaf

Potential application of artificial intelligence to the alpha and gamma radiation from agricultural byproducts used as building and construction materials

Solomon Oyebisi [a,*], Thamer Alomayri [b]

[a] Department of Civil Engineering, Covenant University, PMB 1023, Km 10, Idiroko Road, Ota, Nigeria
[b] Department of Physics, Faculty of Applied Science, Umm Al-Qura University, 21955, Makkah, Saudi Arabia

ARTICLE INFO

Article history:
Received 6 November 2022
Revised 14 March 2023
Accepted 4 July 2023

Editor by: DR B Gyampoh

Keywords:
Alpha radiation
Artificial intelligence
Gamma radiation
Good health and well-being
Responsible consumption and production
Sustainable cities and communities

ABSTRACT

Recycled agricultural wastes are being used in the building and construction sector as cement additives as a result of the environmental impact of cement production. Agricultural byproducts, on the other hand, are naturally occurring radioactive elements that could expose people and the environment to radiation dangers. As a result, this research assesses the radiological characteristics of agricultural byproducts utilized as building and construction materials with special attention to their activity concentrations (^{226}Ra series, ^{232}Th series, and ^{40}K isotopes). The levels of alpha and gamma radiation were measured via the activity concentrations. Alpha and gamma radiation (output data) and activity concentrations (input data) were trained using artificial intelligence techniques, and the model's effectiveness was evaluated. In terms of the metrics of the model, the linear regression algorithm outperformed other algorithms. Finally, none of the agricultural byproducts studied are at risk from alpha and gamma radiation. Thus, the findings provide the reference information needed to build a framework for radiation monitoring of surveyed agricultural byproducts.

Introduction

The production of cement demands high energy and emits high carbon dioxide into the atmosphere [1]. Due to the chemical processes involved in converting limestone-based raw materials into cement clinker, roughly 110 kwh of electricity are used and 0.8 tons of carbon dioxide are released into the atmosphere for every ton of cement produced [2–5]. As a result, there is a possibility for lowering the emissions of carbon dioxide in the form of substituting agricultural waste ashes for cement [3,6,7]. Several agricultural waste products, including rice husk ash [8,9], cashew nut shell ash [10–12], shea nut shell ash [13], corn cob ash [14–16], sugarcane bagasse ash [7,17], coconut shell ash [18], rice straw ash [19], wood ash [20], coconut fiber ash [21,22], egg shell powder [22], groundnut husk ash [23], and others, have been used in the manufacture of sustainable concrete with promising results as a partial replacement for cement. However, agricultural waste ashes utilized as building and construction materials are considered naturally occurring radioactive materials (NORMs), which, in very little amounts, can be dangerous for the environment and human health [24–29].

* Corresponding author. Department of Civil Engineering, Covenant University, PMB 1023, Km 10, Idiroko Road, Ota, Nigeria.
E-mail address: solomon.oyebisi@covenantuniversity.edu.ng (S. Oyebisi).

https://doi.org/10.1016/j.sciaf.2023.e01792

Radiation is energy from radioactively decaying unstable atoms that travels from its source as energy waves or electrified particles [29–31]. Ionizing radiation and non-ionizing radiation are the two categories of radiation, according to the United States Environmental Protection Agency (USEPA) [29]. The energy of non-ionizing radiation is sufficient to move the atoms inside a molecule, but insufficient to expel the electrons from atoms. Microwaves, visible light, and radio waves are some examples. Although ionizing radiation such as x-rays, alpha, beta, and gamma rays possess sufficient energy to take electrons from atoms [29]. Ionizing radiation affects human atoms and poses a health risk by damaging tissues and deoxyribonucleic acid (DNA) in genes [29]. The heaviest radioactive elements including uranium, radium, and polonium decay to produce alpha particles, which are released as alpha radiation. Consequently, the exposure's effects on health through inhalation, ingestion, or physical contact through cuts are dangerous [29],[29].[29] The primary radiation sources in building materials are naturally occurring radionuclides (NORs), particularly the potassium (^{40}K) isotope and the radium (^{226}Ra) and thorium (^{232}Th) series [24–28]. This is supported by pertinent research, which revealed that the primary sources of human exposure to ^{226}Ra, ^{232}Th, and ^{40}K are found in building and construction materials [32–34]. The radiation from ^{226}Ra, ^{232}Th, and ^{40}K's short-lived offspring radionuclides is absorbed by more than 85% of the world's population. In the constructed environment, these radionuclides continuously decay [28,35,36]. Therefore, from the perspective of alpha and gamma radiation, it is crucial to work toward assessing and forecasting the radiological health risk of building inhabitants. However, despite extensive research on the radioactivity of materials, no accurate modeling of the alpha and gamma radiation of agricultural wastes used as construction materials based on artificial intelligence has been done.

Artificial intelligence (AI) is a general term for technology that develops intelligent systems and inspires human intellect to complete a task or achieve a goal through adaptable transformation [37]. To this purpose, it is imperative to stress the use of AI concepts and methodologies in science, technology, engineering, and management, particularly for the prediction of material properties, which can save time and resources [38]. Machine learning algorithms (MLAs), one of the subsets of AI, are gaining popularity in scientific and technological discourse due to their artificial intelligence that resembles the neurons in the human brain. From data sets, it constructs a system and produces patterns and correlations between various components and groups of factors that would be challenging to carry out [39]. Numerous studies have used machine learning algorithms of AI to forecast strength and develop concrete mixes. These include Ensemble Trees (ET), Linear Regression (LR), Regression Trees (RT), Support Vector Machine (SVM), Gaussian Process Regression (GPR), and Artificial Neural Networks (ANN) [40–47]. Some of these applications offer quick estimation and have improved efficiency and precision. The AI of MLA's use in medicine with high accuracy on a dataset with complex reports is another crucial component of the technology [48,49]. Despite the extensive research on artificial intelligence, no study has used AI to foresee alpha and gamma radiation from agricultural outputs; this is why this current study is conducted.

This study emphasizes the specialized functions of agricultural byproducts while providing a thorough review of them. The alpha and gamma rays were evaluated using the activity concentrations. Additionally, the alpha radiation data was trained and tested based on ^{226}Ra utilizing the SVM, ANN, ET, RT, GPR, and LR of machine learning algorithms, whereas the gamma-ray data was trained and evaluated based on three input components (^{226}Ra, ^{232}Th, and ^{40}K). K-fold validation was applied to prevent overfitting and underfitting. The best algorithm for predicting the alpha and gamma radiation of agricultural byproducts was chosen by comparing the performance parameters of each MLA with one another. As a result, these findings aid in the identification and forecasting of radiation dangers to human health for people living in buildings made with these byproducts. Additionally, it suggests employing agricultural byproducts that contain naturally occurring radionuclides and gives the reference data for creating a framework for radiation monitoring.

Dataset

The electronic source, Science Direct and Web of Science, yielded a dataset. The two most dependable and powerful databases for data collection are Web of Science and Science Direct [50]. Identification of other keywords, including "agricultural byproducts," "building materials," and "construction materials", were also searched. To optimize data collection, pertinent NORM data were acquired from United Nations Scientific Committee on the Effects of Atomic Radiation (UNSCEAR), Naturally Occurring Radioactivity in the Nordic Countries (NORDIC), European Commission (EC), and the Canadian Nuclear Safety Commission (CNSC). By carefully locating, evaluating, examining, and reading the articles and references, the data dependability and repeatability were regulated and validated. Superfluous documents were removed using a variety of filtering strategies. The ^{226}Ra, ^{232}Th, and ^{40}K are the input parameters. The target variables (alpha radiation and gamma radiation), also known as the prediction factors, are reliant on the input values.

Radiation

Alpha index (Iα)

The radon-induced alpha radiation that building materials create is determined by the alpha index. Building materials are affected by radon exhalation, which results in an indoor concentration of more than 200 Bq m^{-3} and a specific activity of ^{226}Ra (CRa, Bq kg^{-1}) greater than 200 Bq kg^{-1} [51–53]. However, with a specific activity of ^{226}Ra below 100 Bq kg^{-1}, radon exhalation could not produce an indoor concentration above 200 Bq m^{-3}. Nordic [51] therefore advises the specific activity of ^{226}Ra below 100 Bq kg^{-1} and excludes the upper limit. But the upper limit of 200 Bq kg^{-1} was agreed upon by

Table 1
Alpha and gamma radiation and AEDV ranges.

I_α and I_γ	AEDV ($mSvy^{-1}$)	Material types	Remark
≤ 0.5	0.3	Bulky	Satisfactory material
≤ 1	1	Bulky/Building	Good material
≥ 1	≥ 1	Superficial	Unsuitable material

both the European Commission (EC) [54] and the International Commission on Radiation Protection (ICRP) [55]. Therefore, Eq. (1) [27,54-62] provides the alpha index:

$$I_{\propto} = \frac{C_{Ra}}{200\ Bq\ kg^{-1}} \leq 1 \tag{1}$$

Gamma index (Iγ)

Given that the activity concentrations (C) of ^{226}Ra, ^{232}Th, and ^{40}K have the same gamma dose rates of 300 Bq kg^{-1}, 200 Bq kg^{-1}, and 3000 Bq kg^{-1}, respectively, the gamma index is proposed to analyze and control exposure to gamma radiation (gamma rays) produced from the NORMs [35,36,54]. As a result, Eq. (2) provides the relationship between the gamma index and the activity concentrations (2):

$$I_{\gamma} = \frac{C_{Ra}}{300\ Bq\ kg^{-1}} + \frac{C_{Th}}{200\ Bq\ kg^{-1}} + \frac{C_{K}}{3000\ Bq\ kg^{-1}} \leq 1 \tag{2}$$

Table 1 shows the relationship between radiation indices from building materials and annual equivalent dose values (AEDV) [24,28,36,54,63,64]. The value of alpha and gamma radiation from naturally occurring radioactive elements is clearly a maximum of unity as shown by Eqs. (1) and (2). When the maximum values of alpha and gamma radiation, which correspond to an AEDV of 0.3 and 1 mSvy-1, respectively, are reached, a material is stated to be appropriate for use. However, any material with an AEDV more than 1 mSvy-1 and an alpha and gamma radiation value more than 1 is considered unsuitable for usage [54].

Artificial intelligence

Advanced statistical modeling, machine learning, and deep learning are all subfields of artificial intelligence [37,65]. This study makes use of a machine learning technique since it has been used to model a large number of publications that have been published on concrete manufacturing that includes recycled agro-industrial wastes, yielding high precision [38,46,47,66-72]. An accurate prediction or result is provided by a machine learning algorithm (MLA), which learns input parameters without the need for explicit programming [73]. Since the model is trained using the input variables, the input parameters are referred to as training data [42]. For this investigation, the input data for gamma-ray data were ^{226}Ra, ^{232}Th, and ^{40}K, and ^{226}Ra for alpha. Then, the alpha and gamma indexes were selected as the target variables. Then, using MATLAB R2021a version 9.10.0 1,602,886, machine learning algorithms such as ANN, ET, GPR, LR, RT, and SVM were applied. These algorithms were used because they provide more effectiveness, strong precision, high tolerance for erroneous data, and quick estimation for a variety of modeling tasks [40,41,43-45]. Additionally, the radiation was trained, verified, and tested using SVM, ANN, ET, LR, RT, and GPR machine learning algorithms utilizing three input variables for gamma-ray (^{226}Ra, ^{232}Th, and 40 K) and two for alpha (^{226}Ra). The algorithm with the best performance metrics was identified through comparison of these MLAs. Fig. 1 displays the entire process.

The initial data set in machine learning is split into training and test sets. To fit the model, a portion of the original dataset is used for training, while the full dataset is used for testing the model's correctness. Good training data are hence the basis of machine learning. The model must therefore be trained using high-quality, pertinent, consistent, uniform, and comprehensive data [42]. Overfitting and underfitting issues, however, are the most frequent difficulties with the machine learning model. When a model overfits because it can't effectively generalize to the new data set, its accuracy, performance, and efficiency suffer. In contrast, underfitting happens when a model is unable to recognize the fundamental trend in the data set. As a result, Kim [73] contended that generalizing a model created via MLA is necessary to avoid overfitting and underfitting by lengthening the model's training period or increasing the number of variables in the data set. In order to avoid data overfitting, data validation is necessary. The model's performance is typically validated and enhanced to achieve this using a cross-validation procedure (a 10-fold) [39-45,73,74]. The bias brought on by the random sampling of the training set is reduced by this method. It was used for the meta-analysis and compares the efficacy of several expected modeling strategies. Another key element is the fact that 10-fold cross-validation evenly divides the real datasets into 10 subsets, improves learning with 9 subgroup, and confirms the model with 1 subgroup [75–77]. After completing the process successfully 10 times, an accuracy of 10 times on average is acquired. According to Kohavi [76], the 10-fold cross-validation method exemplifies the generalizability and dependability of model performance.

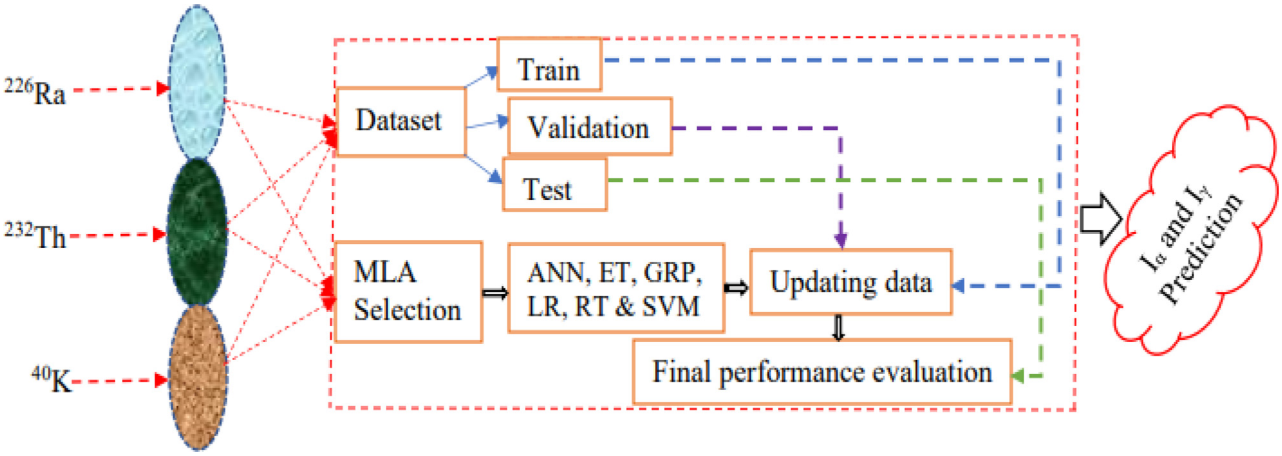

Fig. 1. Machine learning algorithms framework for predicting alpha and gamma radiation.

This work used 10-fold cross-validation to achieve higher model performance by generalizing an independent dataset. All used methods are supervised machine learning algorithms that can accurately predict all input data used as training. To the fullest extent possible, 24 sub-techniques from 6 various supervised machine learning algorithms were used in this investigation. Nevertheless, the most effective results from each supervised machine learning were identified.

The effectiveness of any algorithm is gauged using performance indicators, also called error metrics. As a result, calculating the error rate between the predicted and real variables is crucial for the effectiveness of the MLA employed. This study employed the R^2, MAE, MSE, and RMSE as its four different error measures. The strength of the prediction increases with R^2. However, the accuracy of the prediction improves with decreasing MAE, MSE, and RMSE [78]. The error metrics are given in Eqs. (3)-(6):

$$R^2 = 1 - \frac{\sum_{i=1}^{n}\left(y_i^{pred} - y_i^{true}\right)^2}{\sum_{i=1}^{n}\left(y_i^{pred} - \overline{y^{true}}\right)^2} \tag{3}$$

$$MAE = \frac{1}{n}\sum_{i=1}^{n}\left(y_i^{pred} - y_i^{true}\right) \tag{4}$$

$$MSE = \frac{1}{n}\sum_{i=1}^{n}\left(y_i^{pred} - y_i^{true}\right)^2 \tag{5}$$

$$RMSE = \sqrt{\frac{1}{n}\sum_{i=1}^{n}\left(y_i^{pred} - y_i^{true}\right)^2} \tag{6}$$

Results and discussion

Agricultural byproducts

Due to the dearth of research on the radiological characteristics of recycled agricultural wastes, only rice husk ash (RHA), mussel shell, palm oil clinker (POC), and palm oil fuel ash (POFA) were retrieved from the electronic sources. Their radiological characteristics are displayed in Table 2. The results showed that the activity concentrations of the surveyed agricultural byproducts were below the respective world population-weighted averages of 33, 45, and 420 Bq kg^{-1} for ^{226}RA, ^{232}Th, and ^{40}K [35,36]. In contrast, RHA, POC, and POFA's ^{40}K weighted averages were 16.83%, 28.08%, and 6.04% greater than the global population-weighted averages [35,36]. However, the weighted-average of 500 Bq kg^{-1} for ^{40}K recommended by EC [54] and NEA-OECD [61] was met. All byproducts showed similar results, with alpha and gamma radiation levels below 1, as suggested by UNSCEAR [35,36].

Table 2
Radiological properties of agricultural byproducts studied.

Material	C (Bq kg^{-1}) ^{226}Ra	^{232}Th	^{40}K	Iγ	Iα	Reference
RHA	6	16	505	0.27	0.03	Sas et al. [79]
Average	6	16	505	0.27	0.03	
MS	14.1	8.5	137	0.14	0.07	Alam et al. [80]
MS	9.9	6.1	96.2	0.10	0.05	Alam et al. [80]
MS	9.8	5.7	69.8	0.08	0.05	Alam et al. [80]
MS	12.2	5.6	110	0.11	0.06	Alam et al. [80]
MS	8.8	5.3	105	0.09	0.04	Alam et al. [80]
MS	8.4	4.4	81.4	0.08	0.04	Alam et al. [80]
MS	0.5	1.3	198	0.07	0.00	Krmpotic et al. [81]
MS	8.5	4.7	389	0.18	0.04	Krmpotic et al. [81]
MS	2.0	2.3	188	0.08	0.01	Krmpotic et al. [81]
MS	5.7	6.9	377	0.18	0.03	Krmpotic et al. [81]
Average	7.99	5.08	175	0.11	0.04	
POC	6.89	4.46	571	0.24	0.03	Karim et al. [82]
POC	6.90	4.63	571	0.24	0.03	Karim et al. [82]
POC	5.85	4.40	573	0.24	0.03	Karim et al. [82]
POC	7.01	4.87	599	0.24	0.04	Karim et al. [82]
POC	5.56	4.21	604	0.24	0.02	Karim et al. [82]
POC	6.23	4.76	587	0.24	0.03	Karim et al. [82]
Average	6.41	4.56	584	0.24	0.03	
POFA	8.16	6.14	441	0.20	0.04	Karim et al. [82]
POFA	7.74	6.41	450	0.21	0.04	Karim et al. [82]
POFA	7.95	7.13	457	0.21	0.04	Karim et al. [82]
POFA	8.75	7.98	421	0.21	0.04	Karim et al. [82]
POFA	9.03	7.56	498	0.23	0.05	Karim et al. [82]
POFA	6.98	6.91	413	0.19	0.03	Karim et al. [82]
Average	8.10	7.02	447	0.21	0.04	
Global	33	45	420	≤ 1	≤ 1	*UNSCEAR [35,36]

* UNSCEAR: United Nations Scientific Committee on the Effects of Atomic Radiation.

These findings suggest that alpha and gamma radiation from these byproducts (RHA, MS, POC, and POFA) do not provide a concern to people who utilize them. As a result, with caution, they can be used as construction materials.

(World Population-Weighted Average Value).

Machine learning algorithms of artificial intelligence

The performance metrics for gamma and alpha radiation for each of the six different machine learning techniques are shown in Tables 3 and 4. Six trained algorithms using 24 different models generated test and validation outputs. Comparing the linear regression technique to other algorithms, Table 3 demonstrates clearly that it produced the best metrics for predicting the gamma rays of agricultural byproducts. The outcomes from the stepwise and robust linear regression techniques had the lowest RMSE, MSE, and MAE, as well as 100% R^2 among the linear regression models. When it came to test error, the stepwise linear regression method excelled as well. Table 4 illustrates the performance metrics for the linear regression method that showed the best ability to predict the alpha radiation.

Willmott and Matsuura [78] argued that error scales-for which MAE is a useful generalization of the extent of errors-are responsible for the variation in values. This claims that different models are compared and assessed using MAE based on how well they handle errors. As a result, Table 3's results revealed that LR (interaction) technique performance metrics were 73.56%, 40.50%, 84.85%, 14.19%, and 68.16% more error-free for validating datasets than those of RT (fine trees), SVM (linear), ET (boosted trees), GPR (squared exponential), and ANN (wide) techniques, respectively. The gamma ray testing of agricultural byproducts using the LR technique was also 76.71%, 38.76%, 79.19%, and 3.71% more accurate than using the RT (fine trees), SVM (linear), ET (boosted trees), and GRP (squared exponential) algorithms. However, ANN (wide) outperformed LR method by 76.71% in terms of testing error.

Table 4 demonstrates that the LR, GRP, and ANN achieved similar performance metrics for validating and testing the datasets used to estimate the alpha radiation of agricultural products. But when compared to other algorithms, the LR (robust) method was 60.25%, 29.86%, and 68.17% more accurate for validating the expected outputs than RT (fine trees), SVM (linear), and ET (bagged trees) approaches. The LR (robust) approach also produced performance measures that were 30.10%, 28.04%, and 62.30% more accurate than those of the RT (fine trees), SVM (linear), and ET (bagged trees) algorithms for testing datasets of agricultural byproducts. One factor that contributed to the LR algorithm's superior performance metrics was the linear correlation between activity concentrations and activity concentration indices (gamma and alpha radiation). Therefore, compared to RT, SVM, ET, and GPR, the LR algorithm, a subset of artificial intelligence, delivers perfect regression when used to predict alpha and gamma radiation from agricultural byproducts. After analyzing the literature, it was found

Table 3
Performance metrics for machine learning algorithms used in predicting gamma rays from agricultural byproducts.

MLA	Validation results						Test results				Model
	RMSE	R^2	MSE	MAE	Pred. time (obs/*sec*)	Training time (*sec*)	RMSE	R^2	MSE	MAE	
LR	0.0047258	1.00	0.0000223	0.0038532	240	7.3013	0.0037906	1.00	0.00001437	0.0031470	Linear
	0.0033464	1.00	0.0000180	0.0035311	480	1.3950	0.0033464	1.00	0.00001120	0.0027757	Interaction
	0.0047564	1.00	0.0000226	0.0038833	490	2.097	0.0037913	1.00	0.00001437	0.0031474	Robust
	0.0044895	1.00	0.0000202	0.0037609	410	3.0923	0.0033573	1.00	0.00001127	0.0027694	Stepwise
RT	0.0177370	0.93	0.0003146	0.0133540	460	3.4588	0.0157150	0.94	0.00024697	0.0119200	Fine tree
	0.0687150	0.00	0.0047218	0.0612040	320	0.9184	0.0653710	0.00	0.00427330	0.0578830	Medium tree
	0.0687150	0.00	0.0047218	0.0612040	730	0.7775	0.0653710	0.00	0.00427330	0.0578830	Coarse tree
SVM	0.0081136	0.99	0.0000658	0.0059349	430	2.3007	0.0055962	0.99	0.00003132	0.0045321	Linear
	0.0095539	0.99	0.0000913	0.0079161	640	0.8010	0.0079116	0.99	0.00006259	0.0072201	Quadratic
	0.0150340	0.95	0.0002260	0.0114800	700	0.8138	0.0079815	0.99	0.00006370	0.0070985	Cubic
	0.0467010	0.54	0.0021809	0.0348680	560	0.8166	0.0096385	0.98	0.00009290	0.0094871	Fine gaussian
	0.0294700	0.82	0.0008685	0.0161210	480	1.6116	0.0080667	0.98	0.00006507	0.0072406	Medium gaussian
	0.0287630	0.82	0.0008273	0.0197800	430	0.7307	0.0167790	0.93	0.00028152	0.0128280	Coarse gaussian
ET	0.0289110	0.82	0.0008359	0.0233100	170	5.6624	0.0167170	0.93	0.00027946	0.0133350	Boosted trees
	0.0519570	0.43	0.0026995	0.0431080	210	3.8397	0.0543060	0.52	0.00020526	0.0381760	Bagged tress
GPR	0.0048762	0.99	0.0000238	0.0041151	490	2.7398	0.0034376	1.00	0.00001182	0.0028825	Squared exponential
	0.0076174	0.99	0.0000580	0.0053750	680	0.9090	0.0034270	1.00	0.00001174	0.0028699	Matern 5/2
	0.0194780	0.92	0.0003794	0.0094158	710	0.9672	0.0000365	1.00	0.00000000	0.0000296	Exponential
	0.0048762	0.99	0.0000238	0.0041151	520	1.3103	0.0034376	1.00	0.00001182	0.0028825	Rational quadratic
ANN	0.0462930	0.55	0.0021430	0.0262900	340	7.5464	0.0009995	1.00	0.00000010	0.0007025	Narrow
	0.0721010	−0.1	0.0051985	0.0317830	630	1.5909	0.0009888	1.00	0.00000010	0.0006564	Medium
	0.0172000	0.94	0.0002959	0.0110910	620	1.1963	0.0009872	1.00	0.00000010	0.0006466	Wide
	0.0477630	0.52	0.0022813	0.0239780	540	2.0047	0.0009818	1.00	0.00000010	0.0007172	Bilayered
	0.0912730	−0.8	0.0083308	0.0330390	470	1.8822	0.0009816	1.00	0.00000010	0.0007909	Trilayered

Table 4
Performance indicators of machine learning algorithms used in predicting alpha radiation from agricultural products.

	Validation results						Test results				
MLA	RMSE	R^2	MSE	MAE	Pred. time (obs/*sec*)	Training time (*sec*)	RMSE	R^2	MSE	MAE	Model
LR	0.0031574	0.96	0.0000010	0.0024833	210	7.2911	0.0029373	0.96	0.00000863	0.0023250	Linear
	0.0031574	0.96	0.0000010	0.0024833	650	1.0447	0.0029373	0.96	0.00000863	0.0023250	Interaction
	0.0031441	0.96	0.0000010	0.0024918	590	1.8010	0.0029391	0.96	0.00000863	0.0023097	Robust
	0.0031574	0.96	0.0000010	0.0024833	490	2.0911	0.0029373	0.96	0.00000863	0.0023250	Stepwise
RT	0.0092089	0.65	0.0000848	0.0062681	550	6.7771	0.0059709	0.83	0.00003565	0.0033043	Fine tree
	0.0156390	−0.0	0.0002446	0.011829	890	0.7998	0.0146280	0.00	0.00021399	0.0108880	Medium tree
	0.0156390	−0.0	0.0002446	0.011829	840	0.6228	0.0146280	0.00	0.00021399	0.0108880	Coarse tree
SVM	0.0044552	0.92	0.0000199	0.0035525	590	1.7987	0.0039842	0.93	0.00001587	0.0032097	Linear
	0.0076903	0.76	0.0000591	0.0050221	580	0.9553	0.0061755	0.82	0.00003814	0.0050390	Quadratic
	2.5864000	–	6.6895000	1.0667000	580	10.049	3.0869000	–	9.52900000	2.2971000	Cubic
	0.0144420	0.15	0.0002086	0.0090161	550	1.0352	0.0102330	0.51	0.00010472	0.0057172	Fine gaussian
	0.0122240	0.39	0.0001494	0.0069724	650	0.8894	0.0076546	0.73	0.00005859	0.0050248	Medium gaussian
	0.0130940	0.30	0.0001715	0.0103270	620	0.7201	0.0119500	0.33	0.00014281	0.0098602	Coarse gaussian
ET	0.0105960	0.54	0.0001123	0.0083307	220	4.2325	0.0089185	0.63	0.00007954	0.0066254	Boosted trees
	0.0107870	0.52	0.0001164	0.0078278	250	3.1381	0.0086858	0.65	0.00007544	0.0061268	Bagged tress
GPR	0.0034440	0.95	0.0000119	0.0028894	710	2.4187	0.0029296	0.96	0.00000858	0.0023705	Squared exponential
	0.0034183	0.95	0.0000117	0.0028600	850	0.8170	0.0029282	0.96	0.00000857	0.0023617	Matern 5/2
	0.0054209	0.88	0.0000294	0.0036580	810	0.8239	0.0018814	0.98	0.00000354	0.0012627	Exponential
	0.0034440	0.95	0.0000119	0.0028894	660	1.0454	0.0029296	0.96	0.00000858	0.0023705	Rational quadratic
ANN	0.0046784	0.91	0.0000119	0.0028894	710	2.4187	0.0029296	0.96	0.00000858	0.0023705	Narrow
	0.0038211	0.94	0.0000146	0.0029853	670	1.1752	0.0028659	0.96	0.00000821	0.0022130	Medium
	0.0042677	0.93	0.0000181	0.0030763	680	2.4498	0.0009992	1.00	0.00000010	0.0006544	Wide
	0.0058037	0.86	0.0000337	0.0038235	740	2.0616	0.0028640	0.96	0.00000820	0.0021777	Bilayered
	0.0044608	0.92	0.0000199	0.0031713	620	4.4649	0.0019880	0.98	0.00000395	0.0013356	Trilayered

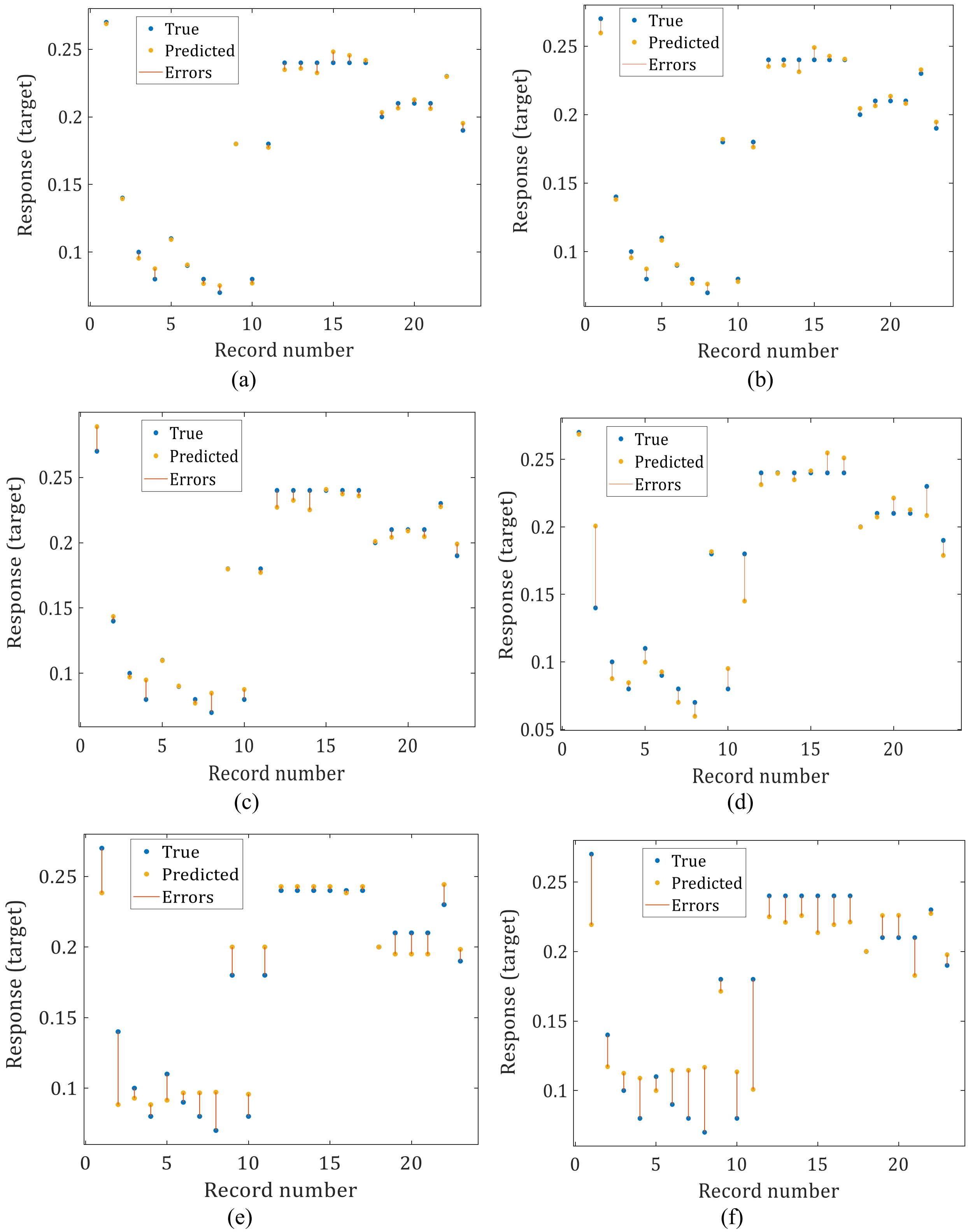

Fig. 2. Response plots for (a) LR (interaction), (b) GPR (squared exponential), (c) SVM (linear), (d) ANN (wide), (e) RT (fine), and (f) ET (boosted) machine learning algorithms for gamma radiation.

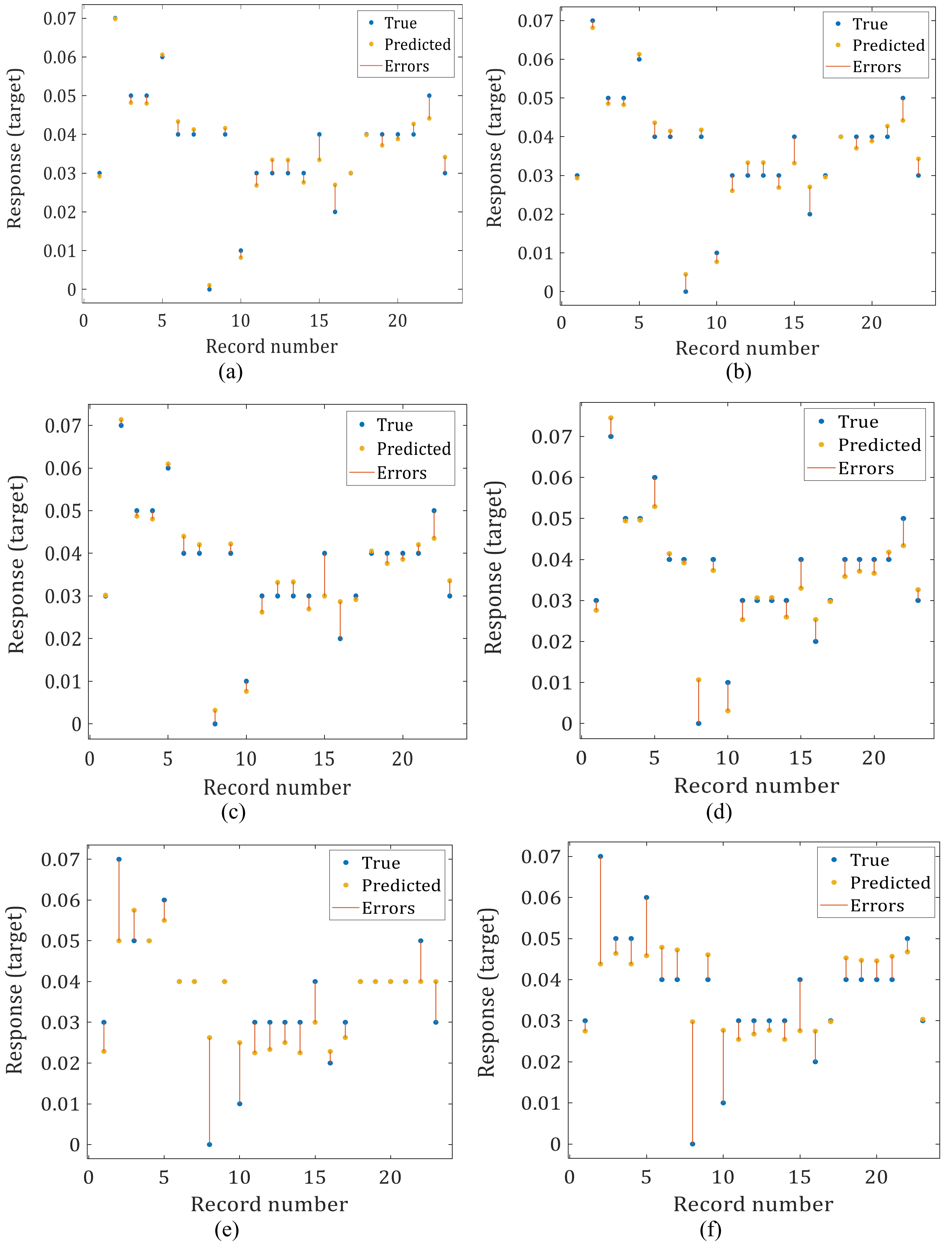

Fig. 3. Response plots for (a) LR (robust), (b) GPR (Matern 5/2), (c) ANN (medium), (d) SVM (linear), (e) RT (fine), and (f) ET (bagged) machine learning algorithms for alpha radiation.

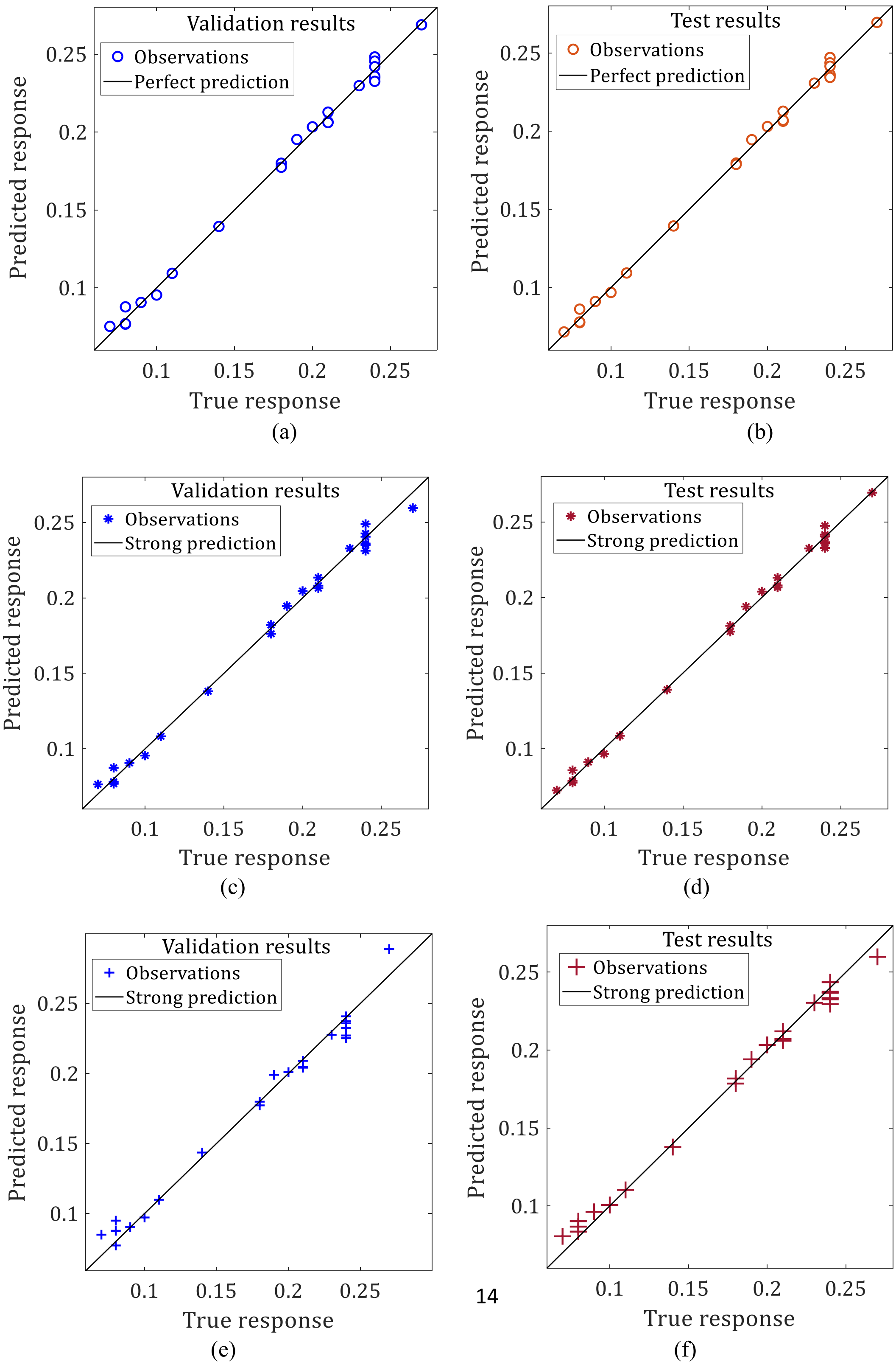

Fig. 4. Predicted versus true responses for (a and b) LR (interaction), (c and d) GPR (squared exponential), (e and f) SVM (linear), (g and h) ANN (wide), (I and j) RT (fine), and (k and l) ET (boosted) machine learning algorithms for gamma radiation.

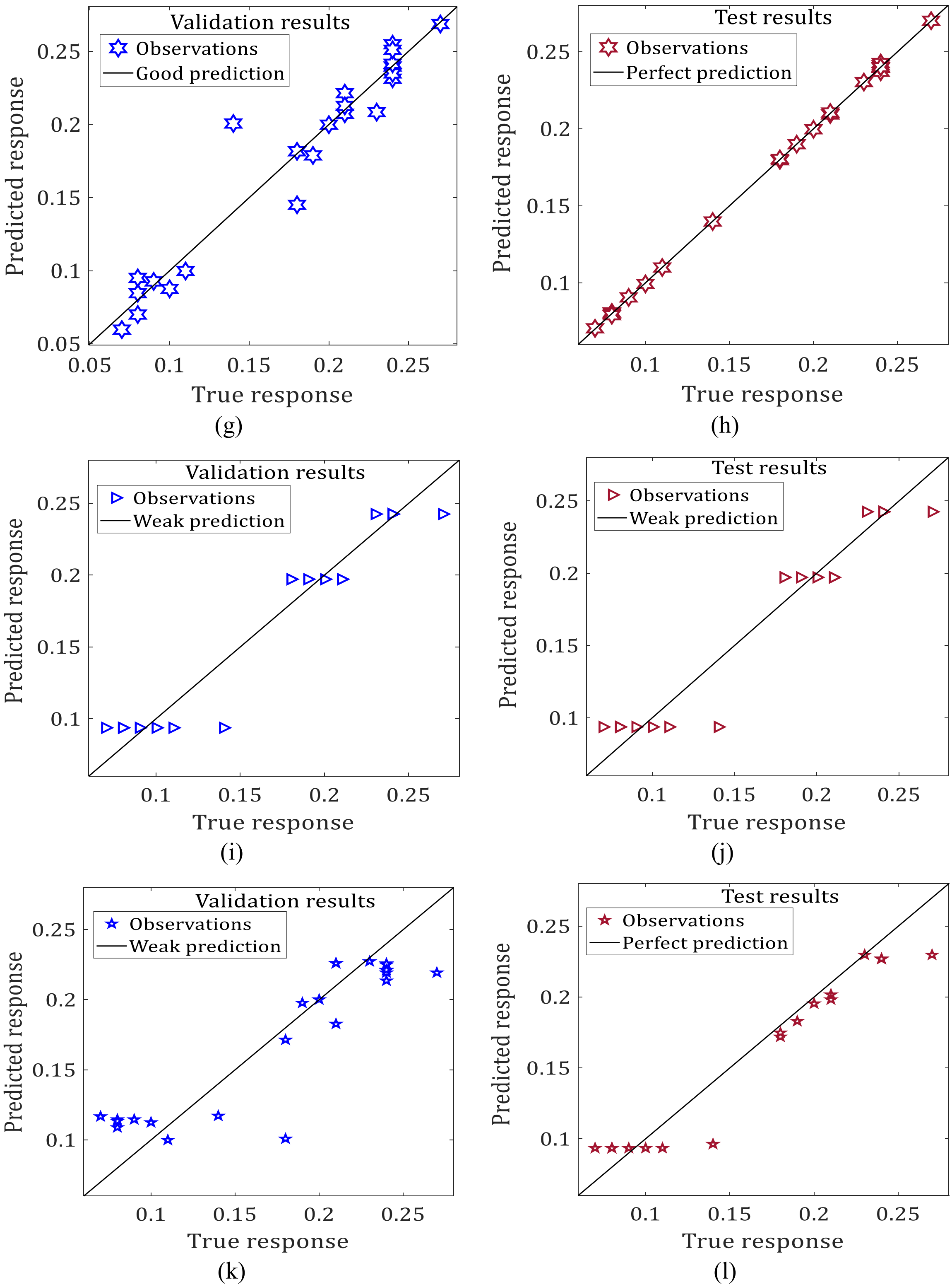

Fig. 4. Continued

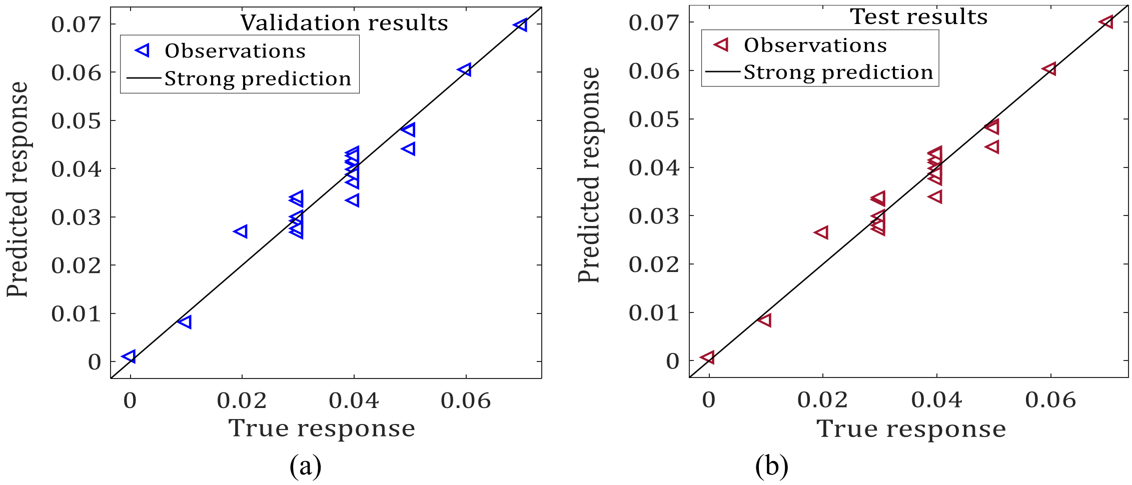

Fig. 5. Predicted versus true responses for (a and b) LR (robust) machine learning algorithms for alpha radiation.

that there was no information on the correlation between activity concentrations and alpha and gamma radiation developed using artificial intelligence approaches. The LR algorithm's results in Tables 3 and 4 nonetheless support Gucluer et al. [83] findings', which found a good correlation between the actual and predicted datasets of concrete's compressive strength.

A model's ability to forecast datasets is, as was previously mentioned, correlated with its R^2 to unity value. As RMSE, MAE, and MSE move closer to zero, the model's performance increases. The performance metrics of MLAs for predicting gamma rays and alpha radiation of agricultural byproducts are provided in Tables 3 and 4. Consequently, these measures demonstrated optimal performance. These performance indicators were LR, ANN, GPR, and SVM, in that order. However, RT and ET produced subpar results.

The response graphs for activity concentrations and record numbers for gamma and alpha radiation are displayed in Figs. 2 and 3, respectively, to highlight the model's performance and response characteristics. For gamma radiation training (Fig. 2), there were 23 observations of the target (response) variable and a total of 69 observations of the input parameters (^{226}Ra, ^{232}Th, and ^{40}K). Also, there were 23 observations of the target parameters and 23 observations of the input variable (^{226}Ra) for alpha radiating training. Every forecast was created using the training model. Unlike RT, ANN, and ET in Figs. 2 and 3, the GPR, LR, and SVM algorithms generated strongly linked responses with little to no error. The radiological properties of the materials, which are influenced by factors such grain sizes, mineral impurities, geological formation and locations, geochemical compositions, and technical processes of industrial byproducts, can be related to the response characteristics [26,32,63,79,84-87].

The predicted vs. true responses of the performance measures for validation and test results are shown in Fig. 4 for gamma radiation, while Fig. 5 shows the best performance algorithm (LR) of alpha radiation. According to the evidence from Fig. 4, all data points of some ML techniques fell on diagonal (regression) lines, signifying a perfect regression model. The response plots created for gamma and alpha radiation in Figs. 2 and 3, and the effectiveness and efficiency of the LR technique are supported by these data. As indicated in Fig. 4, a few datasets using the RT and ET methods, however, showed few outliers, a variety of dispersion, and signs of inaccuracy. Machine learning approaches have not been studied to forecast the gamma and alpha radiation of agricultural byproducts. But it's important to emphasize that these results are consistent with past studies [42,70,75,83], with LR, ANN, SVM, and GPR algorithms yielding an accurate response for the concrete's strengths. These results support the performance metrics for each algorithm presented in Tables 3 and 4.

Figs. 6 and 7 display the model outputs for gamma and alpha radiation using machine learning approaches. The results showed a strong and precise prediction for LR, ANN, GPR, and SVM algorithms since the correlation between the actual and anticipated gamma and alpha radiation equals unity. Additionally, the data perfectly followed the regression line. The ET and RT algorithms, however, occasionally produced outliers, which were data points that were positioned roughly along the regression line. Moreover, the fit line and the target line are not parallel. These results validate the performance indicators shown in Tables 3 and 4, the response plots shown in Figs. 3 and 4, and the highlighted regression graphs shown in Figs. 4 and 5. A comparable output performance was expressed in the modeling of concrete's compressive strength after 28 days of curing by Thilakarathna et al. [42]. The application of LR, ANN, GPR, and SVM approaches generated the model's outputs R values of 85% after training.

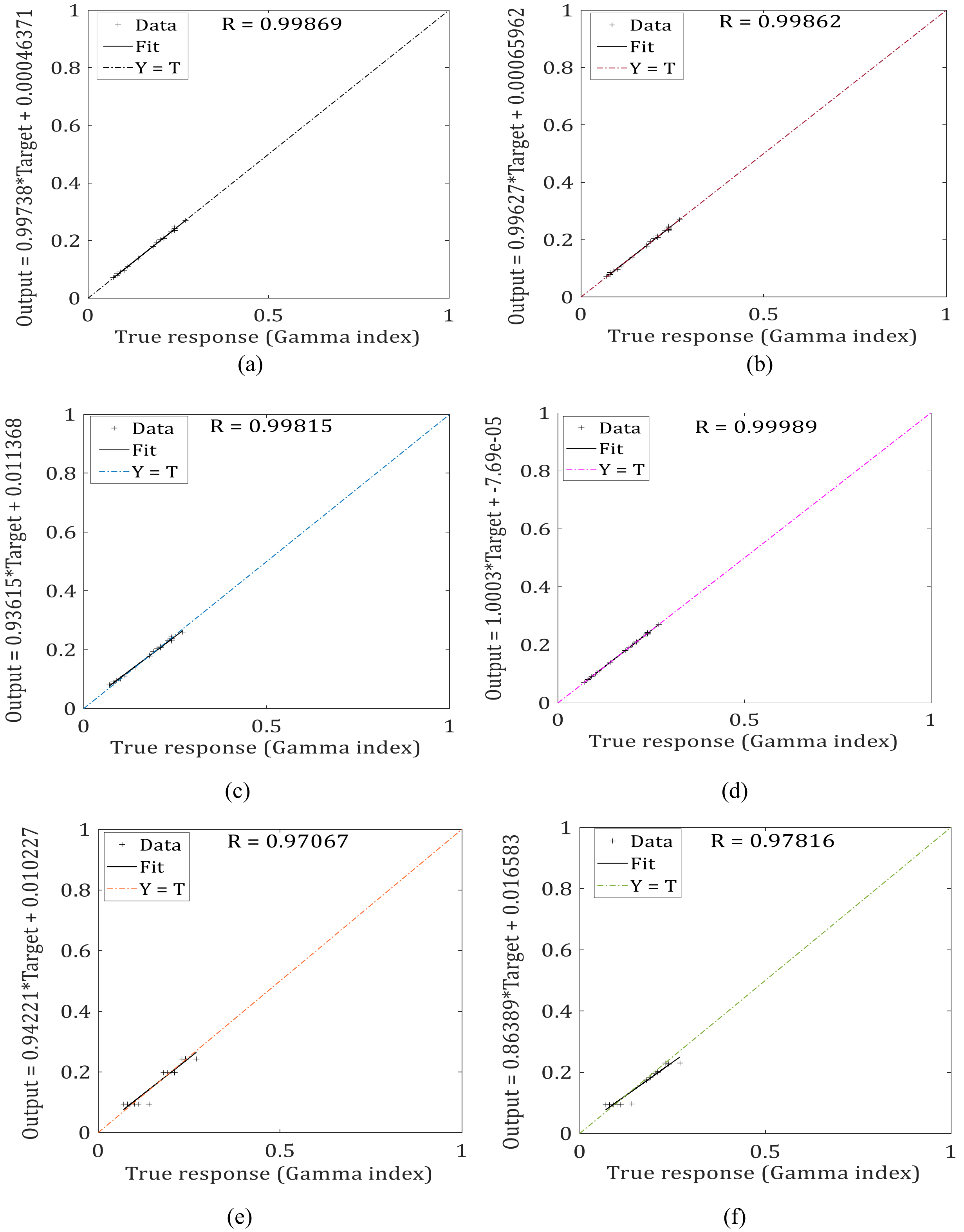

Fig. 6. Model outputs for (a) LR (interaction), (b) GPR (squared exponential), (c) SVM (linear), (d) ANN (wide), (e) RT (fine), and (f) ET (boosted) machine learning algorithms for gamma radiation.

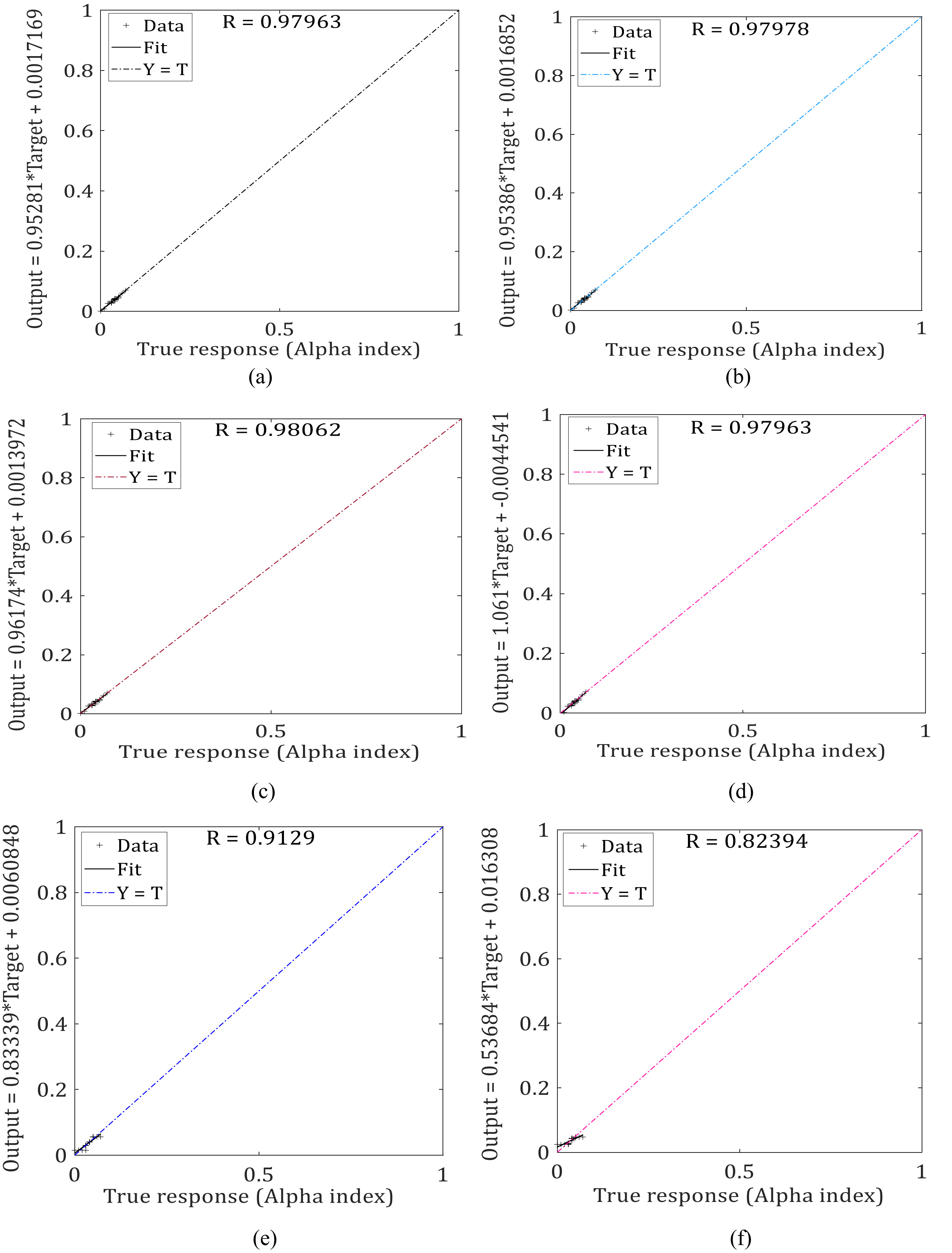

Fig. 7. Model outputs for (a) LR (robust), (b) GPR (Matern 5/2), (c) ANN (medium), (d) SVM (linear), (e) RT (fine), and (f) ET (bagged) machine learning algorithms for alpha radiation.

Conclusions

This current study examined the radiation indexes of agricultural byproducts used as building and construction materials. Moreover, six artificial intelligence of machine learning techniques were engaged to predict the gamma and alpha radiation from these byproducts. Consequently, the following conclusions are drawn from this research:

(a) All surveyed agricultural byproducts pose no alpha and gamma radiation risks.
(b) With the exception of RT and ET, all machine learning techniques for artificial intelligence performed better and had lower disparities between the actual data and the forecasts.
(c) Forecasting the alpha and gamma radiation of the investigated agricultural byproducts with LR showed the highest level of accuracy based on performance metrics.
(d) Compared to GRP, ANN, SVM, RT, and ET algorithms, the mean absolute error of the LR method for validating alpha and gamma radiation was approximately 15–85% lower.
(e) The mean absolute error of the LR approach was between 4 and 80% less than that of the GRP, ANN, SVM, RT, and ET techniques in terms of testing performance.
(f) MLAs of artificial intelligence achieved output performance in the following order after validating and testing datasets for alpha and gamma radiation: LR > GPR > SVM > ANN > RT > ET.

There is currently little to no research that makes predictions on the alpha and gamma radiation of agricultural products using machine learning methods of artificial intelligence. This study filled this knowledge gap and showed that machine learning methods may be used to forecast the alpha and gamma radiation of agricultural byproducts based on ^{226}Ra and ^{232}Th series, as well as the ^{40}K isotopes. As a result of this study's identification of alpha and gamma radiation of recycled agricultural wastes, potential consumers are now better informed about these risks, assisting in the achievement of SDGs 3 (good health and wellbeing), 11 (sustainable cities and communities), and 12 (sustainable consumption and production patterns). Regardless of these encouraging results, additional study is necessary to determine the relevance of alpha and gamma radiation by including data on the radiological radiation indexes of other agricultural byproducts.

Declaration of Competing Interest

The authors declare that they have no known competing financial interests or personal relationships that could have appeared to influence the work reported in this paper.

CRediT authorship contribution statement

Solomon Oyebisi: Conceptualization, Data curation, Formal analysis, Funding acquisition, Investigation, Methodology, Resources, Software, Validation, Writing – original draft. **Thamer Alomayri:** Project administration, Writing – review & editing.

Acknowledgment

The authors want to thank the Department of Civil Engineering of Covenant University for enabling environment.

Ethical approval

No human subjects or animals were used in the research for this article.

References

[1] D. Töbelmann, T. Wendler, The impact of environmental innovation on carbon dioxide emissions, J. Clean. Prod. 244 (2020) 118787, doi:10.1016/j.jclepro.2019.118787.
[2] L. Shen, T. Gao, J. Zhao, L. Wang, L. Wang, L. Liu, F. Chen, J. Xue, Factory-level measurements on CO2 emission factors of cement production in China, Renew. Sustain. Energy Rev. 34 (2014) 337–349, doi:10.1016/j.rser.2014.03.025.
[3] O.F. Arbelaez Perez, D.R. Florez, L.M. Zapata Vergara, K.V. Hernández Benavides, Innovative use of agro-waste cane bagasse ash and waste glass as cement replacement for green concrete. Cost analysis and carbon dioxide emissions, J. Clean. Prod. 379 (2022) 134822, doi:10.1016/j.jclepro.2022.134822.
[4] L.K. Turner, F.G. Collins, Carbon dioxide equivalent (CO2-e) emissions: a comparison between geopolymer and OPC cement concrete, Constr. Build. Mater. 43 (2013) 125–130, doi:10.1016/j.conbuildmat.2013.01.023.
[5] S. Nie, J. Zhou, F. Yang, M. Lan, J. Li, Z. Zhang, Z. Chen, M. Xu, H. Li, J.G. Sanjayan, Analysis of theoretical carbon dioxide emissions from cement production: methodology and application, J. Clean. Prod. 334 (2022) 130270, doi:10.1016/j.jclepro.2021.130270.
[6] A.A. Raheem, B.D. Ikotun, Incorporation of agricultural residues as partial substitution for cement in concrete and mortar – a review, J. Build. Eng. 31 (2020) 101428, doi:10.1016/j.jobe.2020.101428.
[7] B.S. Thomas, J. Yang, A. Bahurudeen, J.A. Abdalla, R.A. Hawileh, H.M. Hamada, S. Nazar, V. Jittin, D.K. Ashish, Sugarcane bagasse ash as supplementary cementitious material in concrete – a review, Mater. Today Sustainab. 15 (2021) 100086, doi:10.1016/j.mtsust.2021.100086.
[8] Z. Syahida Adnan, N.F. Ariffin, S.M. Syed Mohsin, N.H. Abdul Shukor Lim, Review paper: performance of rice husk ash as a material for partial cement replacement in concrete, Mater. Today Proc. 48 (2022) 842–848, doi:10.1016/j.matpr.2021.02.400.
[9] V. Jittin, A. Bahurudeen, S.D. Ajinkya, Utilisation of rice husk ash for cleaner production of different construction products, J. Clean. Prod. 263 (2020) 121578, doi:10.1016/j.jclepro.2020.121578.

[10] S. Oyebisi, T. Igba, D. Oniyide, Performance evaluation of cashew nutshell ash as a binder in concrete production, Case Stud. Construct. Mater. 11 (2019), doi:10.1016/j.cscm.2019.e00293.
[11] S. Oyebisi, T. Igba, A. Raheem, F. Olutoge, Predicting the splitting tensile strength of concrete incorporating anacardium occidentale nut shell ash using reactivity index concepts and mix design proportions, Case Stud. Construct. Mater. 13 (2020), doi:10.1016/j.cscm.2020.e00393.
[12] S. Oyebisi, H. Owamah, T. Alomayri, A. Ede, Modelling the strength of cashew nutshell ash-cement-based concrete, Mag. Concr. Res. 74 (2022), doi:10.1680/jmacr.20.00349.
[13] S. Oyebisi, T. Alomayri, Cement-based concrete modified with Vitellaria Paradoxa ash: a lifecycle assessment, Constr. Build. Mater. 342 (2022), doi:10.1016/j.conbuildmat.2022.127906.
[14] S.O. Oyebisi, F.A. Olutoge, O.M. Ofuyatan, A.A. Abioye, Effect of corncob ash blended cement on the properties of lateritic interlocking blocks, Progr. Indust. Ecol. 11 (2017), doi:10.1504/PIE.2017.092729.
[15] S. Oyebisi, A. Ede, O. Ofuyatan, J. Oluwafemi, I. Akinwumi, Comparative study of corncob ash-based lateritic interlocking and sandcrete hollow blocks, Int. J. GEOMATE 15 (2018), doi:10.21660/2018.51.45918.
[16] D.A. Adesanya, A.A. Raheem, Development of corn cob ash blended cement, Constr. Build. Mater. 23 (2009) 347–352, doi:10.1016/j.conbuildmat.2007.11.013.
[17] I.S. Agwa, A.M. Zeyad, B.A. Tayeh, M. Amin, Effect of different burning degrees of sugarcane leaf ash on the properties of ultrahigh-strength concrete, J. Build. Eng. 56 (2022) 104773, doi:10.1016/j.jobe.2022.104773.
[18] T.C. Herring, T. Nyomboi, J.N. Thuo, Ductility and cracking behavior of reinforced coconut shell concrete beams incorporated with coconut shell ash, Result. Eng. 14 (2022) 100401, doi:10.1016/j.rineng.2022.100401.
[19] I.Y. Hakeem, M. Amin, A.M. Zeyad, B.A. Tayeh, A.M. Maglad, I.S. Agwa, Effects of nano sized sesame stalk and rice straw ashes on high-strength concrete properties, J. Clean. Prod. 370 (2022) 133542, doi:10.1016/j.jclepro.2022.133542.
[20] K. Tamanna, S.N. Raman, M. Jamil, R. Hamid, Utilization of wood waste ash in construction technology: a review, Constr. Build. Mater. 237 (2020) 117654, doi:10.1016/j.conbuildmat.2019.117654.
[21] G.B. Ramesh Kumar, V. Kesavan, Study of structural properties evaluation on coconut fiber ash mixed concrete, Mater. Today Proc. 22 (2020) 811–816, doi:10.1016/j.matpr.2019.10.158.
[22] N. Sathiparan, Utilization prospects of eggshell powder in sustainable construction material – a review, Constr. Build. Mater. 293 (2021) 123465, doi:10.1016/j.conbuildmat.2021.123465.
[23] S. Kumari, R. Walia, Life cycle assessment of sustainable concrete by utilizing groundnut husk ash in concrete, Mater. Today Proc. 49 (2022) 1910–1915, doi:10.1016/j.matpr.2021.08.082.
[24] Council of European Union, Council Directive 2013/59/Euratom of 5 December 2013 laying down basic safety standards for protection against the dangers arising from exposure to ionizing radiation, and repealing directives 89/618/Euratom, 90/641/Euratom, 96/29/Euratom, 97/43/Euratom and 2003/122/Euratom. Off. J. Eur. United Nation, 2014. https://ec.europa.eu/energy/sites/ener/files/documents/CELEX-32013L0059-EN-TXT.pdf (accessed October 20, 2022).
[25] M. Imani, M. Adelikhah, A. Shahrokhi, G. Azimpour, A. Yadollahi, E. Kocsis, E. Toth-Bodrogi, T. Kovács, Natural radioactivity and radiological risks of common building materials used in Semnan Province dwellings, Iran, Environ. Sci. Pollut. Res. 28 (2021) 41492–41503, doi:10.1007/s11356-021-13469-6.
[26] K. Kovler, Radioactive materials, in: toxicity of building materials, Elsevier (2012) 196–240, doi:10.1533/9780857096357.196.
[27] S. Solak, Ş. Turhan, F.A. Uğur, E. Gören, F. Gezer, Z. Yeğingil, İ. Yeğingil, Evaluation of potential exposure risks of natural radioactivity levels emitted from building materials used in Adana, Turkey, Indoor Built Environ. 23 (2014) 594–602, doi:10.1177/1420326×12448075.
[28] United Nations Scientific Committee on the Effects of Atomic RadiationSources and Effects of Ionizing Radiation, United Nations Scientific Committee on the Effects of Atomic Radiation UNSCEAR 2000 Report to the General Assembly, with Scientific Annexes, New York, NY, 2000 accessed October 20, 2022, doi:10.1097/00004032-199907000-00007.
[29] United States Environmental Protection AgencyTechnologically Enhanced Naturally Occurring Radioactive Materials (TENORM), United States, 2022 https://www.epa.gov/radiation/technologically-enhanced-naturally-occurring-radioactive-materials-tenorm accessed October 21, 2022.
[30] E.S. Joel, O. Maxwell, O.O. Adewoyin, O.C. Olawole, T.E. Arijaje, Z. Embong, M.A. Saeed, Investigation of natural environmental radioactivity concentration in soil of coastaline area of Ado-Odo/Ota Nigeria and its radiological implications, Sci. Rep. 9 (2019) 4219, doi:10.1038/s41598-019-40884-0.
[31] O. Maxwell, H. Wagiran, N. Ibrahim, S.K. Lee, Z. Embong, P.E. Ugwuoke, Natural radioactivity and geological influence on subsurface layers at Kubwa and Gosa area of Abuja, Northcentral Nigeria, J. Radioanal. Nucl. Chem. 303 (2015) 821–830, doi:10.1007/s10967-014-3442-1.
[32] E. Kocsis, E. Tóth-Bodrogi, A. Peka, M. Adelikhah, T. Kovács, Radiological impact assessment of different building material additives, J. Radioanal. Nucl. Chem. 330 (2021) 1517–1526, doi:10.1007/s10967-021-07897-4.
[33] R. Mehra, S. Kumar, R. Sonkawade, N.P. Singh, K. Badhan, Analysis of terrestrial naturally occurring radionuclides in soil samples from some areas of Sirsa district of Haryana, India using gamma ray spectrometry, Environ. Earth Sci. 59 (2010) 1159–1164, doi:10.1007/s12665-009-0108-3.
[34] Z. Sas, R. Doherty, T. Kovacs, M. Soutsos, W. Sha, W. Schroeyers, Radiological evaluation of by-products used in construction and alternative applications; Part I. Preparation of a natural radioactivity database, Constr. Build. Mater. 150 (2017) 227–237, doi:10.1016/j.conbuildmat.2017.05.167.
[35] United Nations Scientific Committee on the Effects of Atomic Radiation, Effects of Ionizing Radiation: Report to the General Assembly, With Scientific Annexes, New York, NY, 2008. https://www.unscear.org/docs/publications/2008/UNSCEAR_2008_Report_Vol.I.pdf (accessed October 20, 2022).
[36] United Nations Scientific Committee on the Effects of Atomic RadiationSources and Effects of Ionizing Radiation, United Nations Scientific Committee on the Effects of Atomic Radiation UNSCEAR 2000 Report to the General Assembly, with Scientific Annexes, New York, NY, 1993 https://www.unscear.org/docs/publications/1993/UNSCEAR_1993_Report.pdf accessed October 20, 2022.
[37] M. Haenlein, A. Kaplan, A brief history of artificial intelligence: on the past, present, and future of artificial intelligence, Calif. Manage. Rev. 61 (2019) 5–14, doi:10.1177/0008125619864925.
[38] S.K. Baduge, S. Thilakarathna, J.S. Perera, M. Arashpour, P. Sharafi, B. Teodosio, A. Shringi, P. Mendis, Artificial intelligence and smart vision for building and construction 4.0: machine and deep learning methods and applications, Autom. Constr. 141 (2022) 104440, doi:10.1016/j.autcon.2022.104440.
[39] F.C.B.S.S. Pereira, Machine Learning Fundamentals. In Pereira Big Data and Transport Analytics, Elsevier, Amsterdam, Netherlands, 2019.
[40] G. Bayar, T. Bilir, A novel study for the estimation of crack propagation in concrete using machine learning algorithms, Constr. Build. Mater. 215 (2019) 670–685, doi:10.1016/j.conbuildmat.2019.04.227.
[41] H.M. Mohammed, The determination of ground granulated concrete compressive strength based machine learning models, Period. Eng. Nat. Sci. (PEN) 8 (2020) 1011–1023.
[42] P.S.M. Thilakarathna, S. Seo, K.S.K. Baduge, H. Lee, P. Mendis, G. Foliente, Embodied carbon analysis and benchmarking emissions of high and ultra-high strength concrete using machine learning algorithms, J. Clean. Prod. 262 (2020) 121281, doi:10.1016/j.jclepro.2020.121281.
[43] I.C. Yeh, Modeling of strength of high-performance concrete using artificial neural networks, Cem. Concr. Res. 28 (1998) 1797–1808, doi:10.1016/S0008-8846(98)00165-3.
[44] B.A. Young, A. Hall, L. Pilon, P. Gupta, G. Sant, Can the compressive strength of concrete be estimated from knowledge of the mixture proportions?: new insights from statistical analysis and machine learning methods, Cem. Concr. Res. 115 (2019) 379–388, doi:10.1016/j.cemconres.2018.09.006.
[45] P. Ziolkowski, M. Niedostatkiewicz, Machine learning techniques in concrete mix design, Mater. (Basel) 12 (2019) 1256, doi:10.3390/ma12081256.
[46] Q. Wang, A. Hussain, M.U. Farooqi, A.F. Deifalla, Artificial intelligence-based estimation of ultra-high-strength concrete's flexural property, Case Stud. Construct. Mater. 17 (2022) e01243, doi:10.1016/j.cscm.2022.e01243.
[47] G. Pazouki, Fly ash-based geopolymer concrete's compressive strength estimation by applying artificial intelligence methods, Measurement 203 (2022) 111916, doi:10.1016/j.measurement.2022.111916.

[48] O. İnce, H. Yıldız, T. Kisbet, Ş.M. Ertürk, H. Önder, Classification of retinoblastoma-1 gene mutation with machine learning-based models in bladder cancer, Heliyon 8 (2022) e09311, doi:10.1016/j.heliyon.2022.e09311.
[49] A.W. Olthof, P. Shouche, E.M. Fennema, F.F.A. IJpma, R.H.C. Koolstra, V.M.A. Stirler, P.M.A. van Ooijen, L.J. Cornelissen, Machine learning based natural language processing of radiology reports in orthopaedic trauma, Comput. Method. Program. Biomed. 208 (2021) 106304, doi:10.1016/j.cmpb.2021.106304.
[50] A.A. Chadegani, H. Salehi, M.M. Yunus, H. Farhadi, M. Fooladi, M. Farhadi, N.A. Ebrahim, A comparison between two main academic literature collections: web of science and scopus databases, Asian Soc Sci 9 (2013), doi:10.5539/ass.v9n5p18.
[51] NORDICNaturally Occurring Radioactivity in the Nordic Countries – Recommendations, Norway and Sweden, Denmark, Finland, Iceland, 2000 https://www.gr.is/wp-content/media/2013/07/NaturallyOccurringRadioactivity.pdf accessed October 22, 2022.
[52] R. Ravisankar, K. Vanasundari, A. Chandrasekaran, A. Rajalakshmi, M. Suganya, P. Vijayagopal, V. Meenakshisundaram, Measurement of natural radioactivity in building materials of Namakkal, Tamil Nadu, India using gamma-ray spectrometry, Appl. Radiat. Isot. 70 (2012) 699–704, doi:10.1016/j.apradiso.2011.12.001.
[53] A. Chandrasekaran, R. Ravisankar, G. Senthilkumar, K. Thillaivelavan, B. Dhinakaran, P. Vijayagopal, S.N. Bramha, B. Venkatraman, Spatial distribution and lifetime cancer risk due to gamma radioactivity in Yelagiri Hills, Tamilnadu, India, Egypt. J. Bas. Appl. Sci. 1 (2014) 38–48, doi:10.1016/j.ejbas.2014.02.001.
[54] European Commission, Radiological Protection Principles Concerning the Natural Radioactivity of Building Materials, Radiation Protection Report -RP-112, Luxembourg, 1999. https://ec.europa.eu/energy/sites/ener/files/documents/112.pdf (accessed October 20, 2022).
[55] International Commission on Radiological Protection, Protection against Rn-222 at Home and at Work. ICRP Publication 65, Ann. ICRP 3 (1994) 1–48 https://journals.sagepub.com/doi/pdf/10.1177/ANIB_23_2. accessed October 20, 2022.
[56] M.Y. Shoeib, K.M. Thabayneh, Assessment of natural radiation exposure and radon exhalation rate in various samples of Egyptian building materials, J. Radiat. Res. Appl. Sci. 7 (2014) 174–181, doi:10.1016/j.jrras.2014.01.004.
[57] M.S. Al-Hwaiti, Assessment of the radiological impacts of treated phosphogypsum used as the main constituent of building materials in Jordan, Environ. Earth Sci. 74 (2015) 3159–3169, doi:10.1007/s12665-015-4354-2.
[58] M.U. Khandaker, P.J. Jojo, H.A. Kassim, Y.M. Amin, Radiometric analysis of construction materials using HPGe gamma-ray spectrometry, Radiat. Prot. Dosimetr. 152 (2012) 33–37, doi:10.1093/rpd/ncs145.
[59] M.A. Khatun, J. Ferdous, M.M. Haque, Natural radioactivity measurement and assessment of radiological hazards in some building materials used in Bangladesh, J. Environ. Prot. (Irvine, Calif.) 09 (2018) 1034–1048, doi:10.4236/jep.2018.910064.
[60] M.L. Legasu, A.K. Chaubey, Determination of dose derived from building materials and radiological health related effects from the indoor environment of Dessie city, Wollo, Ethiopia, Heliyon 8 (2022) e09066, doi:10.1016/j.heliyon.2022.e09066.
[61] Nuclear Energy Agency-Organization for Economic Co-operation and Development (NEA-OECD), Exposure to radiation from radioactivity in building materials, 1979.
[62] S. Righi, L. Bruzzi, Natural radioactivity and radon exhalation in building materials used in Italian dwellings, J. Environ. Radioact. 88 (2006) 158–170, doi:10.1016/j.jenvrad.2006.01.009.
[63] K. Aladeniyi, A.M. Arogunjo, A.J.S.C. Pereira, M.U. Khandaker, D.A. Bradley, A. Sulieman, Evaluation of radiometric standards of major building materials used in dwellings of South-Western Nigeria, Radiat. Phys. Chem. 178 (2021) 109021, doi:10.1016/j.radphyschem.2020.109021.
[64] Ş. Turhan, Assessment of the natural radioactivity and radiological hazards in Turkish cement and its raw materials, J. Environ. Radioact. 99 (2008) 404–414, doi:10.1016/j.jenvrad.2007.11.001.
[65] C. Balsano, A. Alisi, M.R. Brunetto, P. Invernizzi, P. Burra, F. Piscaglia, D. Alvaro, F. Bonino, M. Carbone, F. Faita, A. Gerussi, M. Persico, S.J. Santini, A. Zanetto, The application of artificial intelligence in hepatology: a systematic review, Dig. Liver Dis. 54 (2022) 299–308, doi:10.1016/j.dld.2021.06.011.
[66] P.G. Asteris, P.B. Lourenço, P.C. Roussis, C.E. Adami, D.J. Armaghani, L. Cavaleri, C.E. Chalioris, M. Hajihassani, M.E. Lemonis, A.S. Mohammed, K. Pilakoutas, Revealing the nature of metakaolin-based concrete materials using artificial intelligence techniques, Constr. Build. Mater. 322 (2022) 126500, doi:10.1016/j.conbuildmat.2022.126500.
[67] E. Asadi Shamsabadi, N. Roshan, S.A. Hadigheh, M.L. Nehdi, A. Khodabakhshian, M. Ghalehnovi, Machine learning-based compressive strength modelling of concrete incorporating waste marble powder, Constr. Build. Mater. 324 (2022) 126592, doi:10.1016/j.conbuildmat.2022.126592.
[68] M. Sarıdemir, İ.B. Topçu, F. Özcan, M.H. Severcan, Prediction of long-term effects of GGBFS on compressive strength of concrete by artificial neural networks and fuzzy logic, Constr. Build. Mater. 23 (2009) 1279–1286, doi:10.1016/j.conbuildmat.2008.07.021.
[69] B.A. Salami, T. Olayiwola, T.A. Oyehan, I.A. Raji, Data-driven model for ternary-blend concrete compressive strength prediction using machine learning approach, Constr. Build. Mater. 301 (2021) 124152, doi:10.1016/j.conbuildmat.2021.124152.
[70] K.T. Nguyen, Q.D. Nguyen, T.A. Le, J. Shin, K. Lee, Analyzing the compressive strength of green fly ash based geopolymer concrete using experiment and machine learning approaches, Constr. Build. Mater. 247 (2020) 118581, doi:10.1016/j.conbuildmat.2020.118581.
[71] H. Nguyen, T. Vu, T.P. Vo, H.T. Thai, Efficient machine learning models for prediction of concrete strengths, Constr. Build. Mater. 266 (2021) 120950, doi:10.1016/j.conbuildmat.2020.120950.
[72] H. Naseri, H. Jahanbakhsh, P. Hosseini, F. Moghadas Nejad, Designing sustainable concrete mixture by developing a new machine learning technique, J. Clean. Prod. 258 (2020) 120578, doi:10.1016/j.jclepro.2020.120578.
[73] P. Kim, MATLAB Deep Learning, Apress, Berkeley, CA, 2017, doi:10.1007/978-1-4842-2845-6.
[74] D.C. Feng, Z.T. Liu, X.D. Wang, Y. Chen, J.Q. Chang, D.F. Wei, Z.M. Jiang, Machine learning-based compressive strength prediction for concrete: an adaptive boosting approach, Constr. Build. Mater. 230 (2020) 117000, doi:10.1016/j.conbuildmat.2019.117000.
[75] A. Ahmad, W. Ahmad, F. Aslam, P. Joyklad, Compressive strength prediction of fly ash-based geopolymer concrete via advanced machine learning techniques, Case Stud. Construct. Mater. 16 (2022) e00840, doi:10.1016/j.cscm.2021.e00840.
[76] Ron Kohavi, A Study of cross-validation and bootstrap for accuracy estimation and model selection, International Joint Conference on Artificial Intelligence. (1995) 1–7.
[77] H. Song, A. Ahmad, F. Farooq, K.A. Ostrowski, M. Maślak, S. Czarnecki, F. Aslam, Predicting the compressive strength of concrete with fly ash admixture using machine learning algorithms, Constr. Build. Mater. 308 (2021) 125021, doi:10.1016/j.conbuildmat.2021.125021.
[78] Cort J. Willmott, Kenji Matsuura, Advantages of the mean absolute error (MAE) over the root mean square error (RMSE) in assessing average model performance, Clim. Res. 30 (2005) 79–82.
[79] Z. Sas, W. Sha, M. Soutsos, R. Doherty, D. Bondar, K. Gijbels, W. Schroeyers, Radiological characterisation of alkali-activated construction materials containing red mud, fly ash and ground granulated blast-furnace slag, Sci. Total Environ. 659 (2019) 1496–1504, doi:10.1016/j.scitotenv.2019.01.006.
[80] M.N. Alam, M.I. Chowdhury, M. Kamal, S. Ghose, A.K.M.A. Matin, G.S.M. Ferdousi, Radionuclide concentrations in mussels collected from the southern coast of Bangladesh, J. Environ. Radioact. 47 (2000) 201–212, doi:10.1016/S0265-931X(99)00038-7.
[81] M. Krmpotić, M. Rožmarić, D. Barišić, Mussels (Mytilus galloprovincialis) as a bio-indicator species in radioactivity monitoring of Eastern Adriatic coastal waters, J. Environ. Radioact. 144 (2015) 47–51, doi:10.1016/j.jenvrad.2015.02.027.
[82] M.R. Karim, M.U. Khandaker, Kh. Asaduzzaman, H.A. Razak, S.B. Yusoff, Radiological risks assessment of building materials ingredients: palm oil clinker and fuel ash, Indoor Built Environ. 28 (2019) 479–491, doi:10.1177/1420326×18776705.
[83] K. Güçlüer, A. Özbeyaz, S. Göymen, O. Günaydın, A comparative investigation using machine learning methods for concrete compressive strength estimation, Mater. Today Commun. 27 (2021) 102278, doi:10.1016/j.mtcomm.2021.102278.
[84] J. Beretka, P.J. Mathew, Natural radioactivity of australian building materials, industrial wastes and by-products, Health Phys. 48 (1985) 87–95, doi:10.1097/00004032-198501000-00007.

[85] E. Fidanchevski, B. Angjusheva, V. Jovanov, P. Murtanovski, L. Vladiceska, N.S. Aluloska, J.K. Nikolic, A. Ipavec, K. Šter, M. Mrak, S. Dolenec, Technical and radiological characterisation of fly ash and bottom ash from thermal power plant, J. Radioanal. Nucl. Chem. 330 (2021) 685–694, doi:10.1007/s10967-021-07980-w.
[86] R. Trevisi, F. Leonardi, S. Risica, C. Nuccetelli, Updated database on natural radioactivity in building materials in Europe, J. Environ. Radioact. 187 (2018) 90–105, doi:10.1016/j.jenvrad.2018.01.024.
[87] N.M. Hassan, T. Ishikawa, M. Hosoda, A. Sorimachi, S. Tokonami, M. Fukushi, S.K. Sahoo, Assessment of the natural radioactivity using two techniques for the measurement of radionuclide concentration in building materials used in Japan, J. Radioanal. Nucl. Chem. 283 (2010) 15–21, doi:10.1007/s10967-009-0050-6.